HAL open science

Light Polarization in Tunnel Junction Injected UV Light-Emitting Diodes

Jean-Yves Duboz, Victor Fan Arcara, Cynthia Kessaci, Stéphane Vézian, Benjamin Damilano

▶ To cite this version:

Jean-Yves Duboz, Victor Fan Arcara, Cynthia Kessaci, Stéphane Vézian, Benjamin Damilano. Light Polarization in Tunnel Junction Injected UV Light-Emitting Diodes. physica status solidi (a), 2022, 219 (7), pp.2200055. 10.1002/pssa.202200055 . hal-03828269

HAL Id: hal-03828269

https://hal-cnrs.archives-ouvertes.fr/hal-03828269

Submitted on 16 Dec 2022

HAL is a multi-disciplinary open access archive for the deposit and dissemination of scientific research documents, whether they are published or not. The documents may come from teaching and research institutions in France or abroad, or from public or private research centers.

L'archive ouverte pluridisciplinaire **HAL**, est destinée au dépôt et à la diffusion de documents scientifiques de niveau recherche, publiés ou non, émanant des établissements d'enseignement et de recherche français ou étrangers, des laboratoires publics ou privés.

Light polarization in tunnel junction injected UV light emitting diodes

Jean-Yves Duboz[a)], Victor Fan Arcara, Cynthia Kessaci, Stéphane Vézian and Benjamin Damilano

Université Côte d'Azur, CNRS, CRHEA, 06560, Valbonne, France

a) *Corresponding author electronic mail : jyd@crhea.cnrs.fr*

Abstract

The polarization of the light emitted by an ultraviolet light emitting diode has a direct impact on the device performance: a TE polarization of the emission is preferred for extraction from the surface of the diode grown along the c axis. While this is the case for most UV LEDs grown on AlN, this state of events could be called into question when a tunnel junction is added in order to make up for the poor p doping in Al rich (Al,Ga)N and improve the hole injection. Indeed, nitride based tunnel junctions mainly inject holes with a Γ_7 symmetry which could lead to TM polarization of the light emitted by the diode. We have experimentally investigated this important issue and deliver a clear answer to this question.

Ultraviolet (UV) light emitting diodes (LEDs) are currently actively developed for many applications, as can be judged from a recent extensive review[1]. A general problem with nitrides, which has been satisfactorily solved in visible LEDs, is the p doping. For shifting towards the UV range, one has to move from GaN to (Al,Ga)N with an increasing Al content for shorter wavelengths. The Mg acceptor level then becomes deeper and deeper, with a binding energy increasing from 220 meV in GaN to more than 500 meV in AlN[2]. The low hole density in the p region becomes very low (below $10^{16}cm^{-3}$), leading to high access and contact resistances on the p side. Moreover, the imbalance between the electron and hole densities injected in the active region severely degrades the injection efficiency, and *in fine* leads to external quantum efficiencies decreasing with wavelength (see chapter 1 by M. Kneissl in ref. 1). Tunnel junctions (TJs) have been proposed to solve this problem, and demonstrated to be a good solution that does not compromise the hole injection, access resistance and optical transparency. Convincing demonstrations have been reported for nitride visible[3-12] and UV LEDs[13-17] and lasers[18-20]. Another issue in UV LEDs is the polarization of emitted light. Due to the Γ_7- Γ_9 crossover in (Al,Ga)N with increasing Al content, the emission becomes TM polarized in Al rich (Al,Ga)N, which limits its emission through the top surface in structures grown along the c axis[21,22]. While this has been initially thought to be a real limitation in UV LEDs, it has been shown that (Al,Ga)N quantum wells (QW) compressively strained on AlN actually keep a TE polarized emission for emission wavelengths down to 240 nm[23-25]. Due to the strain, the Γ_9 subband remains the fundamental level in these QWs. One question however arises with the use of tunnel junctions: It has been shown that holes injected from the tunnel junction are from the C subband with a Γ_7 symmetry[26]. If these holes injected in the LED quantum well remain with this symmetry, then the emitted light is TM polarized, leading to a reduced photon extraction. In other words, the use of tunnel junction could degrade the extraction efficiency because of the light polarization. The objective of this letter is to precisely address this question.

Interband tunneling in semiconductors was first reported by Esaki[27] in Ge pn junctions and was then described and calculated by many authors[28-30]. The interband tunnel current can be described by an electromagnetic transition between conduction and valence bands under the perturbative action of an electrical field[28,29]. In a semiconductor junction grown along the z direction, the electric field is along z. From symmetry considerations, the corresponding transition is forbidden if the electron and hole wave functions are z independent. In nitrides, the valence band close to Γ is split into three subbands under the joint effects of the spin-orbit and crystal field terms. One subband with Γ_9 symmetry is based on X and Y symmetry wave functions, while the other two of Γ_7 symmetry are based on X, Y and Z symmetry wave functions. The forbidden energy that matters in tunnel processes is about the same when considering all three valence subbands, in particular in GaN and in (In,Ga)N or (Al,Ga)N alloys close to GaN (which are used as interlayers in tunnel junctions) as the crystal field and spin orbit terms are small. Hence the tunnel current is dominated by holes with Γ_7 symmetry. Note that the case of inelastic tunnel current assisted by phonons is not considered here and is expected to be smaller than the elastic tunnel current, when the latter is allowed[29]. In the case of GaN, it was shown that among Γ_7 subbands, the C (spin orbit) band has the largest contribution due to the low hole mass in the C band[26]. One could argue that away from the Γ point, the symmetry is lower and wave functions are mixed up. However, along the z direction, subbands are still based on X,Y and X,Y,Z wave functions. Hence, the tunnel current can be approximated to only generate holes of Γ_7 symmetry.

We can also briefly mention the effect of defects and impurities which may exist at the regrowth interface, in the TJ. Defects break the translation invariance and the parallel k conservation. They may even introduce inelastic processes. However, the tunnel probability will remain larger for split off band holes due to their smaller mass, and the current in the TJ

should remain dominated by holes of Γ_7 symmetry. And finally, it has been shown that the tunnel current is reasonably well described by elastic tunnel current without taking into defects.

When the tunnel junction grown on top of the LED is biased in reverse, holes generated in the p: (Al,Ga)N drift away from the tunnel junction and are injected in the quantum wells of the LED. Even if the hole ground state of the quantum wells has a Γ_9 symmetry, a preferential injection of out-of-equilibrium holes into higher levels with a Γ_7 symmetry could give rise to a light emission mainly polarized along z, i.e. TM polarized. In order to investigate this question, we have compared the polarization of the light emitted by a UV LED without tunnel junction, and the one from the same LED with a tunnel junction. We have designed and fabricated an LED where the TM and TE polarizations are almost equal[31], so that any perturbative effect of the tunnel junction can be observed. We also used a thin p region, as detailed below, and for reasons which will appear clear later on.

The UV-LED was grown on c plane sapphire by metal organic chemical vapor deposition (MOCVD). Details can be found elsewhere[31]. The complete stack consists of a 1000 nm AlN buffer, 1000 nm n-$Al_{0.42}Ga_{0.58}N$ ([Si] = 1×10^{19} cm^{-3}), 3 × [$Al_{0.2}Ga_{0.8}N$ (1.5 nm)/$Al_{0.4}Ga_{0.6}N$ (16 nm)] quantum wells, 20 nm p-$Al_{0.54}Ga_{0.46}N$ electron blocking layer, 50 nm p-$Al_{0.39}Ga_{0.61}N$ ([Mg] = 3×10^{19} cm^{-3}), and a 20 nm p++$Al_{0.39}Ga_{0.61}N$: Mg cap ([Mg] = 1×10^{20} cm^{-3}). This structure underwent an annealing step under N_2 atmosphere after growth to activate the Mg acceptors. Then the tunnel junction was grown by molecular beam epitaxy[31] (to avoid the passivation of Mg acceptors which would occur in MOCVD) and consists of a 3.4 nm GaN interlayer (IL), followed by 25 nm n++ $Al_{0.41}Ga_{0.59}N$ ([Ge] = 5×10^{20} cm^{-3}), 100 nm n+ $Al_{0.41}Ga_{0.59}N$ ([Ge] = 1×10^{20} cm^{-3}), and 10 nm n++ $Al_{0.41}Ga_{0.59}N$ ([Ge] = 5×10^{20} cm^{-3}).

LEDs were fabricated with lateral sizes from 60 to 310 µm. The ohmic n-contacts consist of a stack of Ti/Al/Ni/Au (30/180/40/200 nm, respectively) for the bottom contact of all diodes and the top contact of the TJ-LED, while the ohmic-p contact for LEDs without TJ

consists of a thin Ni/Au (5/5 nm) stack (semitransparent electrode) followed by the deposition of Ni/Au (20/200 nm). Details are given elsewhere[31]. Electro-optical characterizations were realized on wafer under CW conditions at room temperature using a Keithley 2104 source meter and a BWTek spectrometer. The UV emission was collected from the side, from a cleaved edge of the wafer, at an angle of about 5° from the horizontal, by an optical fiber connected to the spectrometer. A UV polarizer (SIGMA KOKI sheet polarizer) was inserted in front of the fiber, so that the distance from the LED to the fiber was about 5 cm, resulting in a low photon collection. Spectra were acquired with a 10 s integration time.

Before measuring the diodes from the side, we also measured them from the back side through the sapphire, as done in a previous work[31], with the UV polarizer. This allowed to check that the detection system (fiber and spectrometer) yields a response independent of the polarization. This measurement was repeated for two positions of the LED, rotated by 90°, to prevent any artefact arising from a possible polarization of the light emitted along the z axis, which could be due to parasitic effects such as the contacts or the mesa edges. In fact, the light emitted along the z axis turned out to be non-polarized as expected from the X-Y symmetry. When rotating the polarizer over 360°, we observed some systematic variations due to non-homogeneities of the polarizer, and which did not indicate any polarization dependence of the detection system. While the spectrometer alone would certainly present such a dependence, the optical fiber depolarizes the light. All in all, the calibration shows that our detection system is polarization independent to better than 4%.

It is also important to assess the ability of our set up to measure the polarization of the light emitted by an LED. While polarization measurements were first done by photoluminescence on the edge of samples[22], measurements on LEDs were more recent and more difficult[32-36]. The difficulty arises because the light is emitted from the entire LED, and reflected on LED edges and contacts. It was shown that the nature of contacts has an impact on

the polarization degree that is measured[34]. It was also shown that the measured degree of polarization is reduced by the light emitted by the top facet and collected at oblique incidence, compared to the degree of polarization that would be measured from the sole LED edge[35]. Most measurements were made without optical imaging system[32-35], and led to polarization ratios (TE/TM) close to 2 and polarization degrees (TE-TM)/(TE+TM) close to 30%. A collecting lens was introduced in order to more exclusively collect light from the LED lateral facet[36]. Polarization degree up to 55% were measured. In order to assess the polarization resolution of our set up, we compared measurements with and without an imaging set up. A collection lens of focal length 10 cm and a diameter of 5 cm (NA=0.25) was used, and the light was focused on the optical fiber by a second lens (20 cm focal length). For this test, we used a blue LED that was expected to be mainly TE polarized, as in ref. 32-35. We measured a polarization degree of 34%. Next we did the measurements without lens, and we found a polarization degree of 28%. We also noted that the polarization degree measured with the lens was more sensitive to alignment details than without lens. As a consequence, we chose to work without lens in order to favor the reproducibility and to ease the comparison between the reference LED and TJ-LED. This preliminary measurements anyhow prove that our set up is qualified to measure the polarization of LEDs.

We first measured EL spectra from the side of the reference LED, without TJ. The lateral size was 300 µm and the current was set to 100 mA, corresponding to about 110 Acm^{-2}. The bias was around 10 V. Fig.1 shows the spectra for both TM and TE polarizations. The spectra are quite noisy due to the low photon collection by the optical fiber, and also because of the low quantum efficiency of our LEDs, in the range of 0.01%, due to the high (> 10^{10} cm^{-2}) dislocation density in the structure[31]. Spectra are similar both in amplitude and peak position. The spectral broadening is about 130 meV.

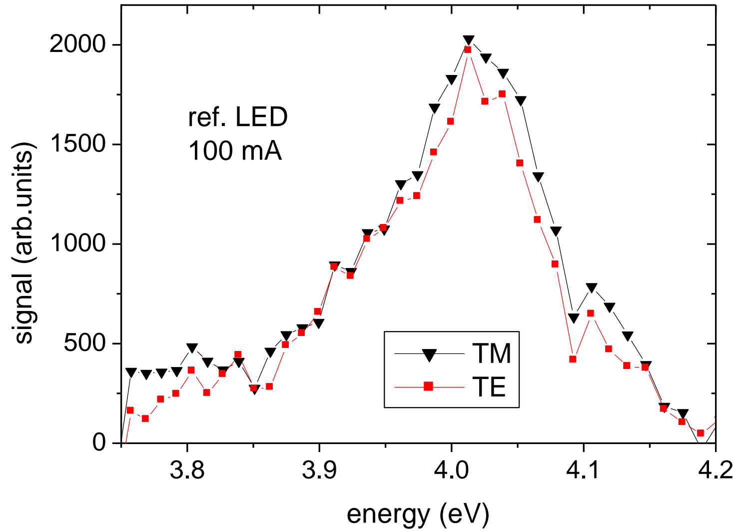

Fig. 1: Electroluminescence spectra measured from the side of the reference LED (without TJ) for TM and TE polarizations, for a current of 100 mA.

A careful analysis as a function of polarizer angle was performed in order to take into account any polarizer non uniformity. We performed a Lorentzian fit of all spectra for various polarization angles. As the peak is asymmetric, the fit was adjusted on the upper part of the peak in order to get a more accurate value of the peak. Let us mention that typical variations of the peak amplitude and energy from one measurement to the next one (for constant parameters) were in the range of 10% and 2 meV respectively. Data shown result from averaging of 2 to 3 measured values. The variation of the peak amplitude with polarization reveals a slight TM polarization, with a TM/TE amplitude ratio around 1.1 (Fig. 2). The peak position deduced from the fit as a function of polarization angle is shown in Fig. 2. The average peak position is about 8 meV lower in energy for TE polarization than for TM polarization. This suggests that the Γ_9 level associated with the TE polarization is slightly lower than the Γ_7 level associated with the TM polarization. The difference between both levels would then be of the order of 8 meV. The

fact that the luminescence intensity is slightly larger in TM polarization, which is not the fundamental level, could arise from differences in the density of states in both subbands. Difference in transmission and scattering at the sample edges for both polarizations could also play a role. We modeled the structure by using NextNano and assuming that the quantum wells are pseudomorphically grown on $Al_{0.42}Ga_{0.58}N$. Using the nominal parameters, we found transition energies of 4.041 eV and 4.051 eV for the transitions associated with the Γ_9 and Γ_7 levels respectively. Both the calculated transition energies and the subband separation agree with the measured values. The exact transition energy (4.02 eV) can be calculated by decreasing the QW Al content by 1% or by increasing its thickness by 0.1 nm, compared to the nominal values. Let us note that the present structure is close to the TE/TM crossover, while the Al content in the QW is 20% only, in contrast with the crossover of 55% Al found in ref. 25. This is because our structure is pseudomorphic on $Al_{0.42}Ga_{0.58}N$, and not on AlN as in ref. 25. It arises because the crystal field depends on strain.

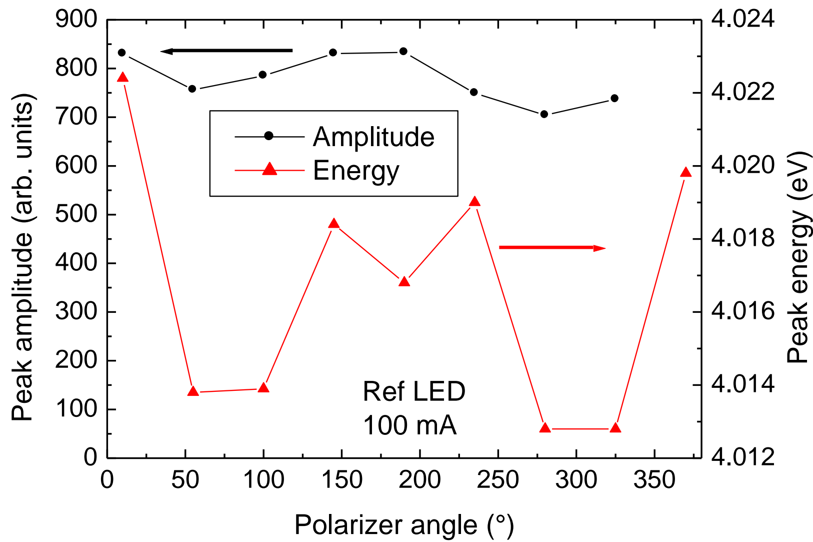

Fig. 2: Peak energy and amplitude of electroluminescence measured from the side of the reference LED (without TJ) as a function of the polarization angle. TM (TE) polarization is obtained for an angle of 10° (100°).

Second, we measured the electroluminescence from the side of the TJ-LED. A smaller diode (60 µm) was used as large diodes tend to fail for an unknown reason. The current was varied from 5 to 25 mA, corresponding to a current density 140 to 1000 Acm^{-2}, with a bias ranging from 12.6 to 14.4 V. The power densities dissipated by this diode are thus larger than the one dissipated by the former reference diode, but due to its smaller size, the actual diode temperature may not be very different in both cases. This will be discussed later on. The electroluminescence spectra measured in TM and TE polarization are shown in Fig. 3 for a current of 5 mA, corresponding to a current density comparable to the one used in Fig. 1.

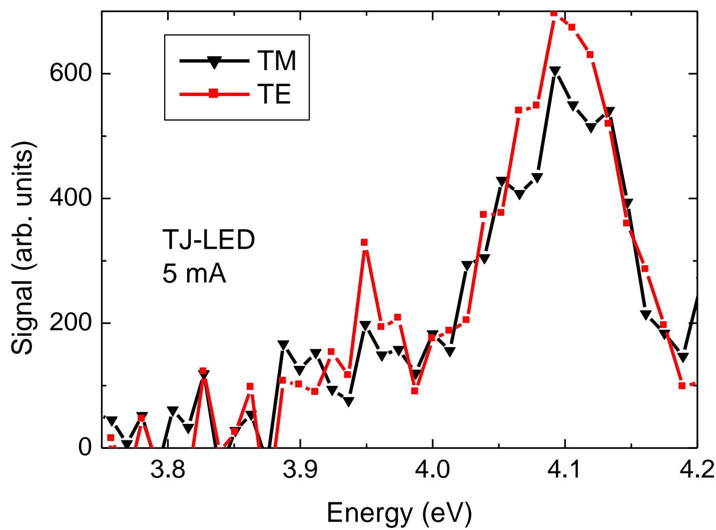

Fig. 3: Electroluminescence spectra measured from the side of the TJ-LED for TM and TE polarizations, for a current of 5 mA.

We observe that the spectra are similar for both polarizations. The signal is larger in TE polarization than in TM by a ratio of 1.15. This ratio remains about the same when the current is increased from 5 to 25 mA (Fig.4).

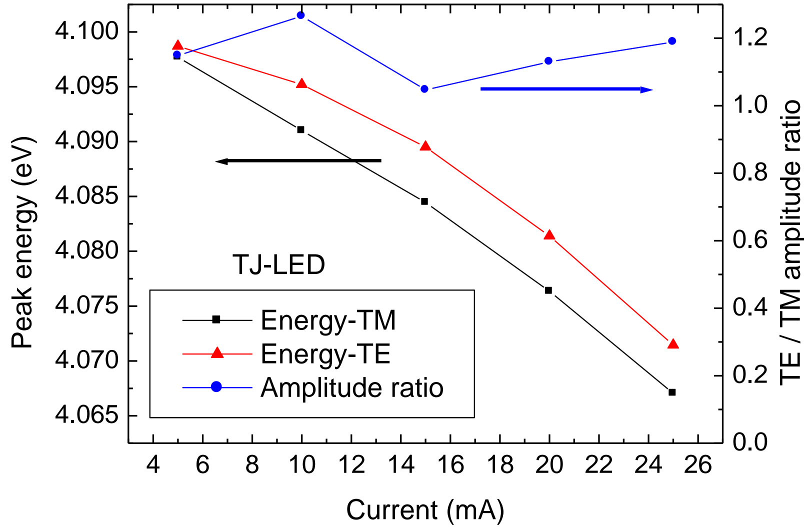

Fig. 4: Energy of the electroluminescence peak in TE and TM polarization, and TE/TM ratio of peak amplitude, as a function of the current for the TJ-LED.

Fitting the peak, we found that the average position of the peak is 5 meV higher in energy in TM than in TE polarization (Fig.4) for all currents (the separation is not well defined for 5 mA due to the limited signal to noise ratio of the spectra and appears smaller). We also found that the energies are larger than in the reference LED, pointing out a slight difference in QW composition, and related to a lateral composition gradient in the LED sample. Modeling indicates that the Al content in the QW might be close to 21% in this diode (versus 20% in the reference LED). The average position of the peak decreases with current due to heating. From the shift of the peak position, and assuming that the band gap energy of (Al,Ga)N varies with temperature as the one of GaN[37], we can estimate a temperature elevation of 50K between 5 and 25 mA. This value, and the slower energy variation around 5 mA indicate that the LED

temperature at a current density of about 140 Acm^{-2} (Fig. 1, 2 and 3) is close to room temperature. We observe that the energy separation between Γ_7 (TM) and Γ_9 (TE) is smaller than in the reference LED (5 versus 8 meV) in agreement with modeling (this separation first decreases when the Al content in the QW increases, and then the subband order is reversed for high quantum well Al contents). We note that the TJ-LED is slightly TE polarized while the reference LED was slightly TM polarized. The slight difference in Al content cannot explain this effect as the lower Γ_7-Γ_9 in the TJ-LED would tend to favor the TM polarization. We have measured different LEDs at various distances from the sample edge to check whether spurious optical effects could affect the result, but could not see any noticeable effect. Hence, we do not have any clear explanation for this small polarization change. However, the important point is that the hole injection from the TJ does not favor the TM polarization, and thus no degradation of the photon extraction has to be feared from the use of tunnel junctions for c-plane UV LEDs.

We previously showed the effect of the TJ on the LED performance[31]. At a constant current, the output power is increased by a factor of about 6 compared to the reference LED, which was interpreted in terms of injection efficiency improved by a better balance between electron and hole currents. Hence, the TJ injects a much larger hole density than a pure p:(Al,Ga)N contact with a Γ_7 symmetry. However, the LED keeps the same emission polarization. This conclusion is of paramount importance for the LED performance. Physically speaking, this result can actually be explained quite simply as follows. The tunnel current in nitride TJ becomes significant when the bias across it becomes a fraction of 1 V, although smaller operating biases can be obtained in optimized TJs[4,5]. Let us take 0.5 V. It has been shown that, for a given total kinetic energy, the tunnel transparency increases when the kinetic energy along z increases[26,29]. The excess energy equal to 0.5 eV (for 0.5 V bias and Fermi levels close to the band edges on the n and p sides) is distributed among the hole and the electron, according to their masses. The calculation[26] shows that holes typically have a kinetic energy along z of 0.2

eV. The transit time, if it would be ballistic, can be estimated from a very rough parabolic approximation of the band and gives a value of 150 fs for an (Al,Ga)N thickness of 100 nm. Holes are mainly injected in the Γ_7 subband. Before reaching the QW, holes may experience scattering, either within the Γ_7 band or towards the Γ_9 subband, if the scattering times are smaller than the ballistic transit time. As the kinetic energy exceeds the LO phonon energy in (Al,Ga)N, scattering includes LO phonon scattering. Acoustic phonon and impurity scattering also come into play. Let us consider first the initial situation where the hole energy exceeds the LO photon energy. Scattering[38-40] within the Γ_7 band is dominated by LO phonons (rate of 8×10^{13} s^{-1}), while deformation potential, piezoelectric effect and impurities all together contribute to a rate of 2×10^{13} s^{-1}, leading to a total scattering rate of 1×10^{14} s^{-1}. Scattering towards the Γ_9 band is dominated by the LO phonons with a rate of 3×10^{14} s^{-1} while the inverse scattering (from Γ_9 to Γ_7) has a smaller rate[38,39] of 1×10^{13} s^{-1}, the difference being due to the density of states in each band. The conclusion is that holes initially in the Γ_7 band rapidly loose energy (within 10 fs) and transfer to the Γ_9 band. When the hole energy has decreased to less than one LO phonon energy, about ¾ of their population has been transferred to the Γ_9 subband. Then, holes with a low energy experience smaller scattering rates as the LO phonon mechanism becomes much slower. Total scattering rates are in the range of 10^{13} s^{-1} both within the Γ_7 subband and from the Γ_7 subband to the Γ_9 subband[39,40], and are thus large enough for scattering to occur before the holes recombine in the QW. Hence, along the transport from the TJ to the QW, the scattering mechanisms between the subbands are fast enough to occur and the population in the QW is governed by the density of states and the thermal Fermi Dirac statistics. The tunnel junction does not modify the population distribution in the QW between subbands, and thus does not affect the photon extraction efficiency.

This proof being obtained on UV LEDs with low efficiencies, one might wonder whether the conclusion remains for high efficiency LEDs. The initial hole population created

by the TJ is redistributed by intersubband relaxation. High efficiency LEDs have dislocation (and other defect) densities much lower than the one in the LED used in this paper, they might thus have a reduced related relaxation rate, and might keep a non-negligible hole population in the split off band. However, as the relaxation is mainly due to LO phonon emission, which does not depend on defects (unless the quality is strongly degraded) this is unlikely. We thus believe that our conclusion will remain true in high efficiency LEDs, but we certainly encourage its verification. We also point out that the p region is quite thin in our structure. LEDs with thicker p regions have an even smaller probability to keep the memory of the hole population injected by the TJ.

As a conclusion, we have experimentally demonstrated that the polarization of the light emitted by a UV LED is not significantly modified by the addition of a tunnel junction. In particular, the TM polarization is not increased respective to the TE polarization, although the holes injected by the tunnel junction mainly have a Γ_7 symmetry. In particular, UVC LEDs grown pseudomorphically on AlN will remain mainly TE polarized even with the addition of a tunnel junction, which is of prime importance for their development and performance.

ACKNOWLEDGEMENTS

We acknowledge support from DUVET (ANR17-CE08-0024) and from GANEX (ANR-11-LABX-0014). GANEX belongs to the public funded 'Investissements d'Avenir' program managed by the French ANR agency. We thank Mathieu Leroux for critical reading of the manuscript.

DATA AVAILABILITY

The data that support the findings of this study are available from the corresponding author upon reasonable request.

REFERENCES

[1]H Amano, R. Collazo, C. De Santi et al, The 2020 UV emitter roadmap, J. Phys. D: Appl. Phys. **53**, 503001 (2020).

[2]B.N. Pantha, J.Y. Lin, and H.X. Jiang, High-Quality Al-Rich (Al,Ga)N Alloys, Ch. 2, 29–82, GaN and ZnO-Based Materials and Devices, Editor S. Pearton (Springer, 2012).

[3]S.-R. Jeon, Y.-H. Song, H.-J. Jang, et al, Appl. Phys. Lett. **78**, 3265 (2001).

[4]S. Krishnamoorthy, D. N. Nath, F. Akyol, et al, Appl. Phys. Lett. **97**, 203502 (2010).

[5]S. Krishnamoorthy, F. Akyol, P. S. Park, et al, Appl. Phys. Lett. **102**, 113503 (2013).

[6]M. Malinverni, D. Martin, and N. Grandjean, Appl. Phys. Lett. **107**, 051107 (2015).

[7]S.-J. Chang, W.-H. Lin, and Ch.-T. Yu, IEEE Electron Device Letters **36**, 366 (2015).

[8]E. C. Young, B. P. Yonkee, F. Wu, et al, Appl. Phys. Express **9**(2), 022102 (2016).

[9]S. Neugebauer, M. P. Hoffmann, H. Witte, et al, Appl. Phys. Lett. **110**, 102104 (2017).

[10]S. J. Kowsz, E. C. Young, B. P. Yonkee, et al, Optics Express **25**, 4, 3841(2017).

[11]J. Wang, E. C. Young, W. Y. Ho, et al, Semiconductor Science and Technology **35**, 125026 (2020).

[12]P. Li, H. Zhang, H. Li, et al, Semiconductor Science and Technology **35**, 125023 (2020).

[13]M. Diagne, Y. He, H. Zhou, et al, Appl. Phys. Lett. **79**, 3720 (2001).

[14]Y. Zhang, S. Krishnamoorthy, J. M. Johnson, et al, Appl. Phys. Lett. **106**, 141103 (2015).

[15]Y. Zhang, S. Krishnamoorthy, F. Akyol, et al, Appl. Phys. Lett. **109**, 191105 (2016).

[16]Y. Zhang, Z. Jamal-Eddine, F. Akyol, et al, Appl. Phys. Lett. **112**, 071107 (2018).

[17]A. Pandey, J. Gim, R. Hovden, et al, Appl. Phys. Lett. **117**, 241101 (2020).

[18]J. T. Leonard, E. C. Young, B. P. Yonkee, et al, Appl. Phys. Lett. **107**, 091105 (2015).

[19]C. A. Forman, S. G. Lee, E. C. Young, et al, Appl. Phys. Lett. **112**, 111106 (2018).

[20]S. G. Lee, C. A. Forman, C. Lee, et al, Applied Physics Express **11**, 062703 (2018).

[21]S. L. Chuang and C. S. Chang, Phys. Rev. B **54**, 2491 (1996).

[22]M. Leroux, S. Dalmasso, F. Natali, et al, Phys. Stat. Sol. (b) **234**, 887 (2002).

[23]R. G. Banal, M. Funato, and Y. Kawakami, Phys. Rev. B **79**, 121308 (R) 2009.

[24]J. E. Northrup, C. L. Chua, Z. Yang, et al, Appl. Phys. Lett. **100**, 021101 (2012).

[25]C. Reich, M Guttmann, M. Feneberg, et al, Appl. Phys. Lett. **107**, 142101 (2015).

[26]J.-Y. Duboz and B. Vinter, J. of Appl. Phys. **126**, 174501 (2019).

[27]L. Esaki, Phys. Rev. **109**, 603 (1958).

[28]E.O. Kane, J. Phys. Chem. Solids **12**, 181 (1959).

[29]E.O. Kane, J. Appl. Phys. **32**, 1, 83 (1961).

[30]L.V. Keldysh, Sov. Phys. JETP **6**, 4, 763 (1958).

[31]V. Fan Arcara, B. Damilano, G. Feuillet, et al, J. of Appl. Phys. **126**, 224503(2019).

[32] X._Du, H. Lu, P. Han, et al, Appl. Phys. Lett. **92**, 203504 (2008)

[33] C. Jia, T. Yu, S. Mu, et al, Appl. Phys. Lett. **90**, 211112 (2007)

[34] L. J. Yan, J. K. Sheu, F. W. Huang, et al, J. Appl. Phys. **108**, 113102 (2010)

[35] M. F. Schubert, S. Chhajed, J. K. Kim, et al, Appl. Phys. Lett. **91**, 051117 (2007)

[36] T. Kolbe, A. Knauer, C. Chua, et al, Appl. Phys. Lett. **97**, 171105 (2010)

[37]H. Teisseyre, P. Perlin, T. Suski, et al, J. of Appl. Phys. **76**, 2429 (1994)

[38]B. C. Lee, N. S. Mansour, Y. M. Sirenko, et al, Semicond. Sci. Technol. **12**, 280 (1997).

[39]J.Y. Duboz, J. of Applied Physics **92**, 4312 (2002).

[40]J. D. Albrecht, P. P. Ruden, and T. L. Reinecke, J. of Applied Physics **92**, 3803 (2002).